METABOLIC STRATEGIES IN *POLYGONATUM*: GROWTH-STRESS TRADE-OFF REVEALED VIA MULTI-OMICS

YIN, L. H. – WANG, X. Z. – XIAO, Q.* – CUI, L. J.

Hubei Key Laboratory of Biological Resources Protection and Utilization, Hubei Minzu University, Enshi 445000, China

**Corresponding author*
e-mail: 1992022@hbmzu.edu.cn; phone: +86-718-843-7326; fax: +86-718-843-7326

(Received 30th Sep 2025; accepted 23rd Dec 2025)

Abstract. As an emerging ideal crop, *Polygonatum* is receiving increasing attention. *Polygonatum kingianum var. grandifolium* (HBES) and *Polygonatum sibiricum* Red (SXHZ) are two *Polygonatum* ecotypes with contrasting traits; HBES shows significantly higher biomass and polysaccharide content than SXHZ. To investigate the underlying molecular mechanisms, a comparative metabolomic and transcriptomic analysis was conducted. The results revealed significant ecotypic differentiation in the organic acid metabolic pathway. HBES exhibited a "growth-type" metabolic pattern, characterized by a marked enrichment of carbon flux into the tricarboxylic acid (TCA) cycle. This was evidenced by increased accumulation of key intermediates. such as succinic acid and α-ketoglutaric acid, supporting highly efficient energy metabolism that fuels robust biomass accumulation and polysaccharide synthesis. In contrast, SXHZ enhanced the shikimic acid pathway, directing carbon flux toward secondary metabolites synthesis and forming a "defense-type" metabolic pattern. This strategy prioritizes stress resistance but also limits biomass production. Transcriptome analysis further identified multiple key genes involved in regulating this differential carbon flow allocation. These distinct carbon allocation strategies are likely stable genetic traits shaped by their native soil environments, ultimately defining the architecture and function of their organic acid metabolic networks. This study, from an organic acid metabolism perspective, reveals critical differences in central carbon metabolism among *Polygonatum* ecotypes, providing a theoretical basis for breeding high-yield, high-resistance varieties.
Keywords: *Polygonatum sibiricum Red, Polygonatum kingianum var. grandifolium, organic acid metabolism, ecotype differentiation, carbon allocation*

Introduction

Polygonatum sibiricum, a perennial herbaceous plant in the Liliaceae family, is a significant medicinal herb in Traditional Chinese Medicine (TCM), with its medicinal properties documented in various historical Chinese materia medica texts. According to the 2020 edition of the Pharmacopoeia of the People's Republic of China, the medicinal material for *Polygonatum* is derived from the dried rhizomes of *Polygonatum kingianum* Coll. et Hemsl., *Polygonatum sibiricum* Red., or *Polygonatum cyrtonema* Hua (Liao et al., 2023).

Polygonatum contains a variety of bioactive compounds, including polysaccharides (Lai et al., 2024), flavonoids (Mo et al., 2024), saponins (Li et al., 2022), and organic acids, which collectively contribute to its pharmacological activities, such as antioxidant (Chen et al., 2024), antibacterial (Azari et al., 2020), anti-inflammatory (Wang et al., 2024), and anti-fatigue effects (Zhang et al., 2024). Organic acids, ubiquitous carboxyl-containing secondary metabolites in plants, are not only key intermediates in the tricarboxylic acid (TCA) cycle but also play central roles in plant energy metabolism, stress response, and signal transduction (Schwachtje et al., 2018). Research has proved that organic acids can enhance plant yield and environmental adaptability (Morgunov et

http://www.aloki.hu ● ISSN 1589 1623 (Print) ● ISSN 1785 0037 (Online)
DOI: http://dx.doi.org/10.15666/aeer/2402_19191936

al., 2017). In *Polygonatum*, organic acids significantly influence its medicinal quality. They do not act in isolation but work synergistically with components such as polysaccharides and flavonoids to constitute the material basis for *Polygonatum*'s efficacy (Ma et al., 2022). Traditional processing methods, such as repeated steaming and sun-drying (Guan et al., 2024), significantly alter the composition of bioactive compounds in *Polygonatum*. This process can reduce the levels of irritating aldehydes and ketones while increasing levels of organic acids, thereby improving taste, reducing irritation, and enhancing therapeutic effects. Regarding antioxidant activity, phenolic acids in processed *Polygonatum* contribute to scavenging free radicals and form a complementary defense network with polysaccharides (Wang et al., 2024). For hypoglycemic effects, organic acids may inhibit intestinal α-glucosidase activity, delaying carbohydrate absorption, while synergizing with polysaccharides to improve insulin resistance, resulting in more sustained, moderate blood glucose regulation (Yu et al., 2024).

Polygonatum sibiricum Red. (SXHZ) is a common variety widely cultivated in Hanzhong City, Shaanxi Province; whereas *Polygonatum kingianum var*. grandifolium (HBES) is a variant primarily distributed in Enshi City, Hubei Province. These two exhibit significant differences in agronomic traits. Compared to SXHZ, HBES demonstrates superior yield and environmental adaptability. Notably, the polysaccharide content in HBES reaches 84.3 mg/g, significantly exceeding the quality standard for ordinary *Polygonatum* (70 mg/g) stipulated by the Pharmacopoeia of the People's Republic of China (Ning et al., 2024). However, the role of organic acids in the growth, development, and metabolic regulation of *Polygonatum* remains unclear. To address this research gap, this study employed an integrated metabolomic and transcriptomic analysis to compare the organic acid composition and biosynthetic pathways in HBES and SXHZ, further constructing an organic acid metabolic network and screening key biosynthetic genes and metabolites.

This research primarily addresses the following important questions: elucidating the genetic differences in organic acid synthesis and accumulation between HBES and SXHZ, screening key functional genes that regulate these differences, and discussing the response mechanisms of organic acid metabolic pathways and their specific contributions to overall quality formation in *Polygonatum*. This study will not only help deepen the understanding of secondary metabolic regulation in *Polygonatum* but also provide a crucial scientific basis for variety selection, standardized cultivation, and improvement of medicinal quality for *Polygonatum* varieties from Shaanxi and Hubei provinces.

Materials and methods

Plant materials

HBES samples were collected from agricultural growers in Laifeng County, Enshi Prefecture, Hubei Province, while SXHZ samples were sourced from agricultural growers in Hanzhong City, Shaanxi Province. All plants were uniformly transplanted in September 2020 to the Medicinal Plant Germplasm Resource Garden of Hubei Minzu University (open field) and cultivated under identical environmental conditions. A mixed substrate of peat and vermiculite at a 1:8 volume ratio was used for cultivation. The plants grew under natural light and temperature conditions and were regularly irrigated to maintain substrate moisture. After three years of growth, their rhizomes were collected in September 2023. Three biological replicates were set for each *Polygonatum* variety,

http://www.aloki.hu ● ISSN 1589 1623 (Print) ● ISSN 1785 0037 (Online)
DOI: http://dx.doi.org/10.15666/aeer/2402_19191936

resulting in a total of six samples. After washing with ultrapure water, the samples were immediately flash-frozen in liquid nitrogen and stored at -80°C. The sample IDs were designated as HBES-M1, HBES-M2, HBES-M3, and SXHZ-M1, SXHZ-M2, SXHZ-M3. All plant materials were identified by Researcher Liao Chaolin from the Institute of Chinese Herbal Medicine, Hubei Academy of Agricultural Sciences, as *Polygonatum kingianum var*. grandifolium and *Polygonatum sibiricum* Red. The authenticated *Polygonatum* specimens are deposited in the Hubei Provincial Key Laboratory for Conservation and Utilization of Biological Resources.

Metabolite extraction and analysis

Metabolite extraction was performed as follows. First, the biological samples were lyophilized using a freeze-dryer (Scientz-100F). The dried material was then ground into a fine powder with a grinding mill (MM 400, Retsch) at 30 Hz for 1.5 min. Subsequently, 50 mg of the powdered sample was accurately weighed and dissolved in 1.2 mL of 70% aqueous methanol extraction solution. The mixture was vortexed for 30 s at 30-min intervals, a total of 6 cycles. After centrifugation at 12,000 rpm for 3 min, the supernatant was carefully collected, filtered through a 0.22 μm microporous membrane, and transferred into an injection vial for subsequent UPLC-MS/MS analysis.

Metabolomics data were acquired using an ultra-performance liquid chromatography (UPLC, SHIMADZU Nexera X2) system coupled to tandem mass spectrometry (MS/MS, Applied Biosystems 4500 QTRAP). Metabolite separation was achieved using an Agilent SB-C18 column (1.8 μm, 2.1 × 100 mm). The mobile phase consisted of ultrapure water containing 0.1% formic acid (A) and acetonitrile containing 0.1% formic acid (B). The gradient elution program was set as follows: starting at 5% B, linearly increasing to 95% B over 9.0 min, holding for 1.0 min, then decreasing to 5% B within 1.1 min, followed by a 14-min equilibration period. Throughout the experiment, the flow rate was maintained at 0.35 mL/min, the column temperature was set at 40°C, and the injection volume was four μL. All LC-MS analyses were conducted by Wuhan Metware Biotechnology Co., Ltd. Mass spectrometric detection utilized an electrospray ionization (ESI) source, operating in both positive and negative ion modes. The ion source temperature was set at 550°C; the spray voltage was 5500 V for positive ion mode (ESI^+) and -4500 V for negative ion mode (ESI^-). The pressures for the nebulizer gas (GS I), auxiliary gas (GS II), and curtain gas (CUR) were set at 50, 60, and 25 psi, respectively. Collision-induced dissociation (CID) was performed using high-sensitivity mode. For data analysis, multivariate statistical analyses including principal component analysis (PCA), partial least squares-discriminant analysis (PLS-DA), and orthogonal partial least squares-discriminant analysis (OPLS-DA) were performed using the ropls R package (Thévenot et al., 2015). Differential metabolites were identified based on the criteria: fold change (FC) > 2 or < 0.5, and variable importance in projection (VIP) > 1. Finally, metabolic pathway enrichment analysis of these differential metabolites was performed using the Kyoto Encyclopedia of Genes and Genomes (KEGG) database (Kanehisa et al., 2023).

RNA extraction and sequencing analysis

Total RNA was extracted from *Polygonatum* rhizomes using the E.Z.N.A.® Plant RNA Kit (R6827, OMEGA, USA). The quality of the extracted RNA was rigorously assessed, and all samples met the following criteria before proceeding to library construction: (1) Agarose gel electrophoresis confirmed intact RNA bands with no

http://www.aloki.hu ● ISSN 1589 1623 (Print) ● ISSN 1785 0037 (Online)
DOI: http://dx.doi.org/10.15666/aeer/2402_19191936

detectable DNA contamination; (2) The Qsep400 High-throughput Nucleic Acid and Protein Analysis System (Ginkgo BioWorks, China) confirmed RNA purity with OD260/280 ratios between 1.8 and 2.0 and OD260/230 ratios greater than 2.0; (3) RNA concentration was accurately quantified using a Qubit 4.0 Fluorometer (Thermo Fisher Scientific, USA); (4) RNA integrity was assessed using an Agilent 2100 Bioanalyzer, requiring an RNA Integrity Number (RIN) > 7.0.

After passing quality control, cDNA libraries were constructed using an automated library preparation workstation (MGI Tech, China) and sequenced on the Illumina platform. Following the acquisition of high-quality clean reads, de novo transcriptome assembly was performed using the Trinity software (Grabherr et al., 2011). After assembly, transcripts were hierarchically clustered using Corset, and the most extended transcript sequence within each resulting cluster was defined as a "unigene", serving as the reference gene set for subsequent analysis.

The unigene sequences were aligned against multiple databases, including KEGG, NCBI non-redundant protein sequences (Nr), Swiss-Prot, Clusters of Orthologous Groups of proteins (COG)/euKaryotic Ortholog Groups (KOG), and TrEMBL, using the BLASTX function of DIAMOND software. Simultaneously, they were aligned against the Pfam database using HMMER to obtain protein domain annotations. Gene Ontology (GO) annotations were acquired based on the results from the aforementioned analyses. Gene expression levels were quantified using FPKM values, and differential expression analysis was performed with DESeq2 (Love et al., 2014).

Transcriptome and metabolome correlation analysis

To identify pivotal genes associated with organic acid biosynthesis, this study performed an integrated analysis. We screened for differentially expressed genes (DEGs) and systematically compared organic acid metabolite accumulation between HBES and SXHZ samples. To explore the regulatory relationships between genes and metabolites in depth, we first identified key gene modules using Weighted Gene Co-expression Network Analysis (WGCNA) and evaluated the correlations between these modules and metabolite accumulation levels (Langfelder and Horvath, 2008). Next, Pearson correlation analysis was performed to calculate pairwise correlation coefficients (r) between all differentially expressed genes (DEGs) and differentially accumulated metabolites (DAMs), with statistical significance assessed using a two-tailed t-test ($p < 0.05$). Finally, based on significantly correlated gene–metabolite pairs ($|r| > 0.8$, $p < 0.05$), an interaction network was constructed and visualized using Cytoscape software (Shannon et al., 2003). Data analysis and visualization were primarily conducted using R software (version 4.2.3) and its associated packages (R Core Team, 2023).

Results

Metabolite analysis of HBES and SXHZ rhizomes

Through qualitative and quantitative analyses of organic acid metabolites in the rhizomes of HBES and SXHZ, we identified 47 organic acids (*Table 1*). Principal component analysis (PCA) revealed clear separation in metabolite composition between the HBES and SXHZ sample groups. In contrast, samples within each group showed high reproducibility and tight clustering, indicating that inter-group differences far exceeded intra-group variations (*Fig. 1A*).

http://www.aloki.hu ● ISSN 1589 1623 (Print) ● ISSN 1785 0037 (Online)
DOI: http://dx.doi.org/10.15666/aeer/2402_19191936

Table 1. *47 organic acids and their related signaling pathways*

Index	Compounds	CAS	cpd_ID	kegg_map
pme3207	Muconic acid	1119-72-8	C02480	ko01100
Zmgn001448	2-Propylmalic acid*	-	C05994	ko00620
Lmbn001754	3-Isopropylmalic acid*	921-28-8	C04411	ko00290, ko01100, ko01110, ko01210, ko01230
MWS1962	cis-Citral	5392-40-5	C09847	ko01110
mws0192	Succinic acid*	110-15-6	C00042	ko00020, ko00190, ko00250, ko00310, ko00350, ko00360, ko00620, ko00630, ko00640, ko00650, ko00760, ko00920, ko01100, ko01110, ko01200
MWSmce210	Chelidonic acid	99-32-1	C08476	-
Zmyn000453	Isocitric acid	320-77-4	C00311	ko00020, ko00630, ko01100, ko01110, ko01200, ko01210, ko01230, ko01240
pme3096	Aminomalonic acid	1068-84-4	C00872	-
mws0275	L-Malic acid	97-67-6	C00149	ko00020, ko00620, ko00630, ko00710, ko01100, ko01110, ko01200
mws0277	Quinic acid	77-95-2	C00296	ko00400, ko01100
pmb3101	2-Isopropylmalic acid	49601-06-1	C02504	ko00290, ko00620, ko01100, ko01110, ko01210, ko01230
pme3017	2-Aminoisobutyric acid	62-57-7	C03665	-
Lmbn001467	5-Acetamidopentanoic acid	1072-10-2	C03087	ko00310, ko01100
Lmbn000216	3-Methylmalic acid*	152204-30-3	C06032	ko00290, ko00660, ko01100, ko01210, ko01230
pme2380	α-Ketoglutaric acid	328-50-7	C00026	ko00020, ko00040, ko00053, ko00220, ko00250, ko00300, ko00310, ko00340, ko00430, ko00630, ko00650, ko00660, ko01100, ko01110, ko01200, ko01210, ko01230, ko01240
mws2125	Phosphoenolpyruvate	138-08-9	C00074	ko00010, ko00020, ko00400, ko00440, ko00620, ko00710, ko00998, ko01100, ko01110, ko01200, ko01230, ko01240
pmf0420	Benzyl acetate	140-11-4	C15513	-
pme0274	6-Aminocaproic acid	60-32-2	C02378	ko01100

http://www.aloki.hu ● ISSN 1589 1623 (Print) ● ISSN 1785 0037 (Online)
DOI: http://dx.doi.org/10.15666/aeer/2402_19191936

Lmbn001288	2-Hydroxy-2-methyl-3-oxobutanoic acid*	71698-08-3	C06010	ko00290, ko00650, ko00660, ko00770, ko01100, ko01110, ko01210, ko01230
MWS1882	Iminodiacetic acid	142-73-4	C19911	-
pmb2826	L-Citramalic acid	6236-09-5	C02614	ko00660, ko01100
mws0281	Citric acid	77-92-9	C00158	ko00020, ko00250, ko00630, ko01100, ko01110, ko01200, ko01210, ko01230, ko01240
Wmzn000227	2,2-Dimethylsuccinic acid	597-43-3	-	-
mws0154	Shikimic acid	138-59-0	C00493	ko00400, ko01100, ko01110, ko01230, ko01240
Zmyn000247	2-Hydroxyglutaric acid*	13095-48-2	C03196	ko00310, ko01100
MWSmce583	Piperonylic acid	94-53-1	-	-
pme1654	Jasmonic acid	77026-92-7	C08491	ko00592, ko01100, ko01110, ko04075
MWS3036	3-Hydroxyglutaric acid	638-18-6	-	-
pme1974	Pyruvic acid	127-17-3	C00022	ko00010, ko00020, ko00030, ko00040, ko00053, ko00250, ko00260, ko00261, ko00270, ko00290, ko00330, ko00350, ko00360, ko00430, ko00440, ko00620, ko00630, ko00650, ko00660, ko00710, ko00730, ko00760, ko00770, ko00900, ko01100, ko01110, ko01200, ko01210,
mws0237	Azelaic acid	123-99-9	C08261	-
Lmmn002164	Monomethyl succinate	3878-55-5	-	-
mws0473	2-Methylsuccinic acid*	498-21-5	-	-
Lmmn000806	Dimethylmalonic acid*	595-46-0	-	-
Lmbn001364	4-Hydroxy-2-Oxopentanoic acid*	3318-73-8	C03589	ko00360, ko01100
Lmmn003323	2-Hydroxyhexadecanoic acid	764-67-0	-	-
Lmsn015919	Phytic acid	83-86-3	C01204	ko00562, ko01100, ko04070
Lmbn000612	1-Pyrroline-4-hydroxy-2-carboxylic acid	9054-77-7	C04282	ko00330, ko01100
mws0567	4-Guanidinobutyric acid	463-00-3	C01035	ko00330, ko01100
MWS0811	L-Pipecolic acid	3105-95-1	C00408	ko00310, ko00960, ko01100, ko01110
Lmtn004049	Abscisic acid	21293-29-8	C06082	ko00906, ko01100, ko01110, ko04075
mws0147	β-Hydroxyisovaleric acid	625-08-1	C20827	ko00280, ko01100

http://www.aloki.hu ● ISSN 1589 1623 (Print) ● ISSN 1785 0037 (Online)
DOI: http://dx.doi.org/10.15666/aeer/2402_19191936

Lmgn000160	3-Ureidopropionic acid	462-88-4	C02642	ko00240, ko00410, ko00770, ko01100
pme3011	γ-Aminobutyric acid	56-12-2	C00334	ko00250, ko00330, ko00410, ko00650, ko00760, ko01100
pme0278	2,6-Diaminooimelic acid	583-93-7	C00666	ko00300, ko01100, ko01110, ko01230
pme3186	DL-Glyceraldehyde-3-phosphate	591-59-3	C00661	-
mws0470	Methylmalonic acid*	516-05-2	C02170	ko00240, ko00280, ko00640, ko01100
mws1039	3-Aminoisobutyric acid	144-90-1	C05145	-

Index is the internal number. Compounds refers to the chemical name; CAS is the globally recognized chemical substance identifier assigned by ACS; cpd_ID is the ID in the KEGG database; KEGG_map indicates the biological metabolic pathways in which the compound is involved

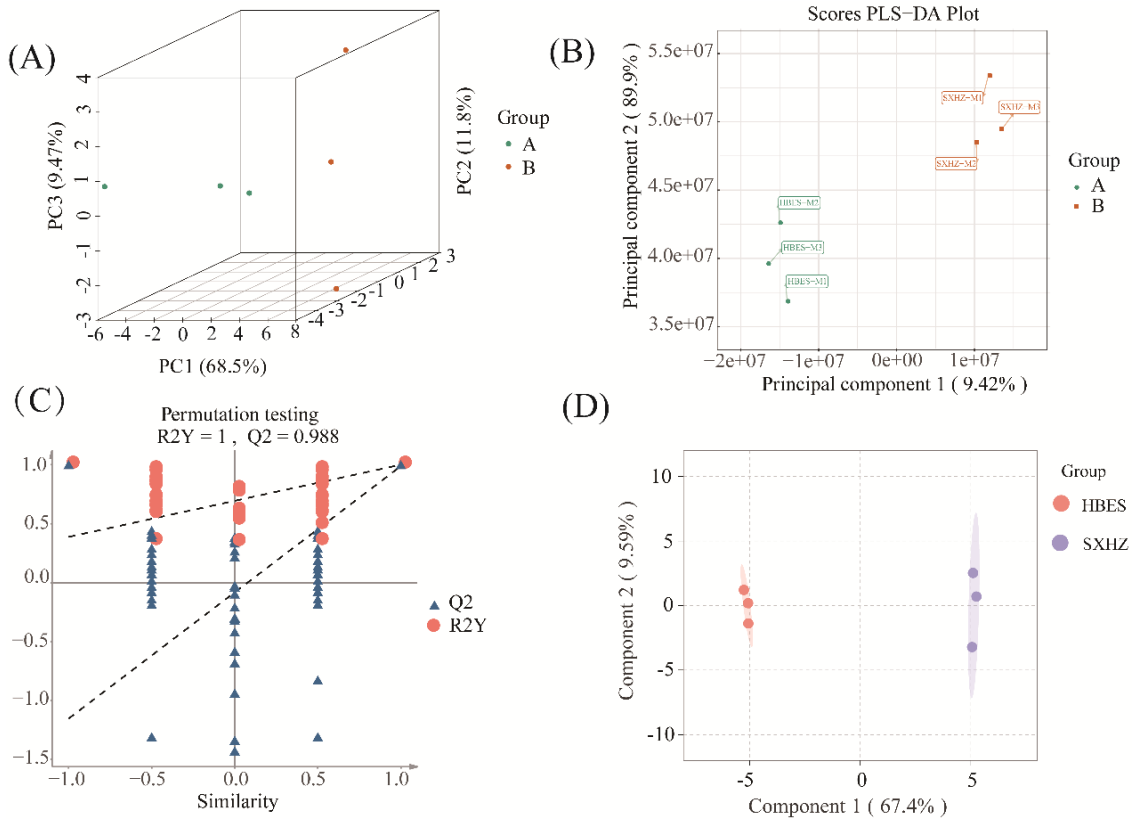

Figure 1. *Multivariate statistical analysis of HBES and SXHZ. (A) overall samples PCA plot; (B) PLS-DA plot; (C) OPLS-DA validation plot; (D) OPLS-DA score plot*

To further distinguish inter-group differences and identify potential metabolites differentially accumulated, we employed supervised orthogonal partial least squares-discriminant analysis (OPLS-DA) and its derivative models. The PLS-DA results demonstrated clear separation of the two sample groups along the first principal component, further supporting the species-specific metabolic profiles of HBES and SXHZ (*Fig. 1B*).

http://www.aloki.hu ● ISSN 1589 1623 (Print) ● ISSN 1785 0037 (Online)
DOI: http://dx.doi.org/10.15666/aeer/2402_19191936

To evaluate model quality and prevent overfitting, we validated the models through cross-validation and response permutation testing. The OPLS-DA model demonstrated excellent performance in both goodness-of-fit (R2Y = 1) and predictive ability (Q2 = 0.988), indicating a stable and reliable model with strong explanatory and predictive power (*Fig. 1C*). Based on this model, we further generated score plots and loading plots to identify metabolites contributing most significantly to group separation, thereby providing a foundation for subsequent screening of differentially accumulated organic acids (*Fig. 1D*).

Analysis of DEMs and enrichment of metabolic pathways

To gain deeper insights into the differences in organic acid metabolism between HBES and SXHZ, we first screened for differentially expressed metabolites (DEMs). In the HBES vs. SXHZ comparison, 19 DEMs were identified, with 8 up-regulated and 11 down-regulated (*Fig. 2C*). The overall expression patterns of the differential metabolites were visualized using hierarchical clustering heatmaps (*Fig. 2A*). The results showed that the HBES-M1, HBES-M2, and HBES-M3 samples clustered into one group, while the SXHZ-M1, SXHZ-M2, and SXHZ-M3 samples clustered into another group. Good intra-group reproducibility and clear inter-group separation were observed, indicating high stability and reliability of the differential metabolites. Meanwhile, distinct relative expression trends across the six sample groups were evident for different metabolites, further confirming significant differences in the organic acid metabolic profiles between HBES and SXHZ.

KEGG enrichment analysis indicated that the DEMs were significantly enriched in pathways such as pyrimidine metabolism, propanoate metabolism, and biosynthesis of secondary metabolites (*Fig. 2B*). Further annotation of DEMs into the four main KEGG categories showed that the “Metabolism” category contained the highest number, with 17 metabolites (*Fig. 2D*). The metabolites showing the most pronounced concentration changes included succinic acid (mws0192) and 1-pyrroline-4-hydroxy-2-carboxylate (Lmbn000612).

Statistical analysis of differentially expressed genes

Through transcriptome analysis, a total of 2599 differentially expressed genes (DEGs) were identified, comprising 1544 up-regulated and 1055 down-regulated genes (*Fig. 3A, B*). To elucidate the potential functions of these genes systematically, we performed Gene Ontology (GO) functional enrichment analysis and Kyoto Encyclopedia of Genes and Genomes (KEGG) pathway enrichment analysis.

The GO enrichment analysis aimed to interpret the biological attributes of the DEGs from a functional perspective. Results revealed significant enrichment in terms such as “carbohydrate metabolic process” and “oxidoreductase activity” (*Fig. 3C*).

Furthermore, KEGG pathway analysis was used to identify the core metabolic and regulatory networks in which these differentially expressed genes participate at the systems level. The results indicated that “Metabolic pathways” and “Biosynthesis of secondary metabolites” were the most significantly enriched pathways (with Q-values approaching zero), highlighting global differences in primary metabolite accumulation and secondary metabolite synthesis between the two varieties. Concurrently, the significant enrichment of pathways such as pyrimidine metabolism, pyruvate metabolism, and sulfur metabolism also suggests their potential key roles in organic acid synthesis and

http://www.aloki.hu ● ISSN 1589 1623 (Print) ● ISSN 1785 0037 (Online)
DOI: http://dx.doi.org/10.15666/aeer/2402_19191936

interconversion (*Fig. 3D*). This analysis not only pinpointed the specific biochemical pathways involving the DEGs but also contextualized their functions within a broader metabolic framework, providing a system-level perspective for understanding the molecular basis of phenotypic differences.

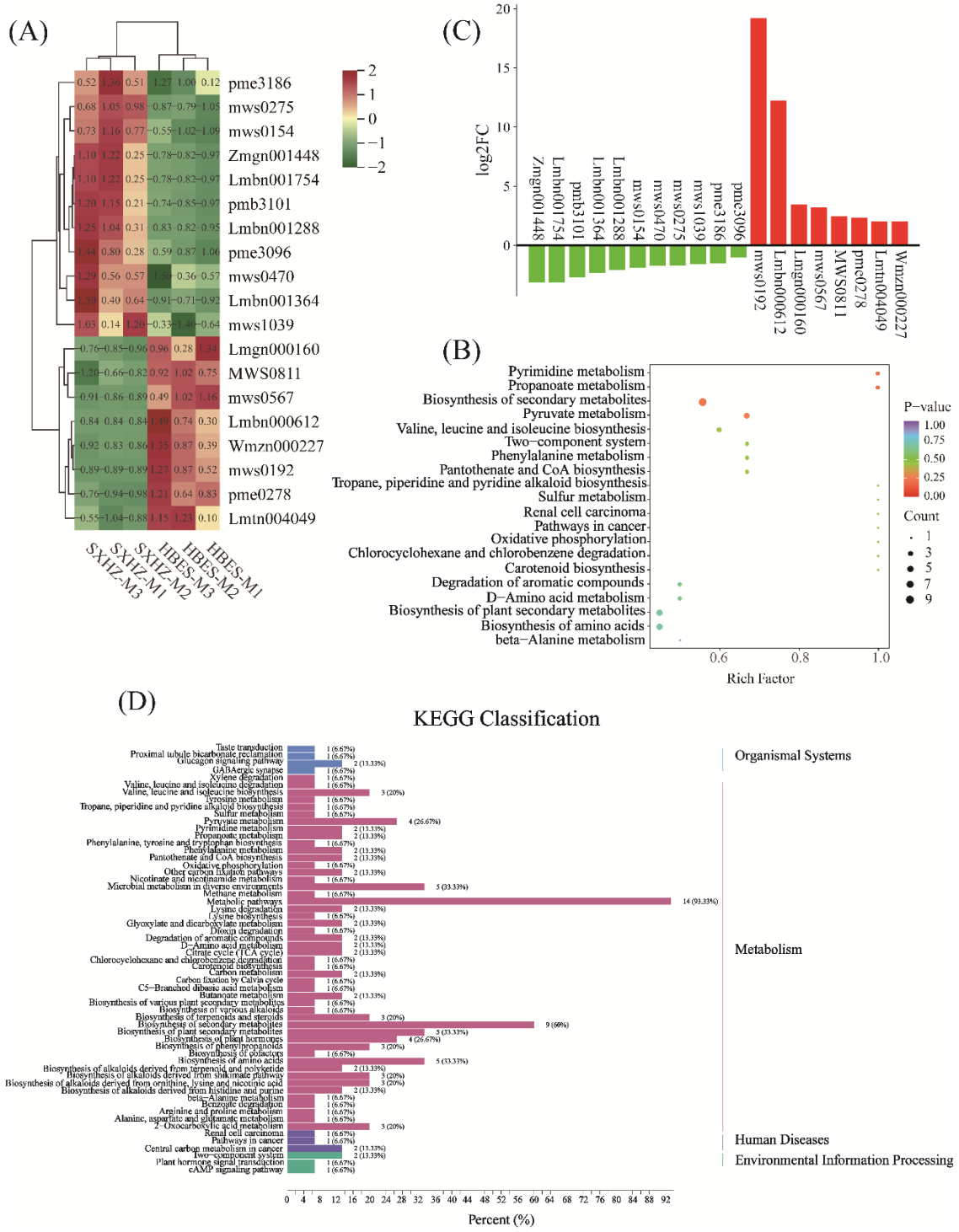

Figure 2. *Analysis of differential metabolites and KEGG data between HBES and SXHZ. (A) Differential metabolite clustering heatmap. (B) Pathway enrichment analysis plot. (C) Significance analysis of differential metabolites plot. (D) Functional classification plot*

http://www.aloki.hu ● ISSN 1589 1623 (Print) ● ISSN 1785 0037 (Online)
DOI: http://dx.doi.org/10.15666/aeer/2402_19191936

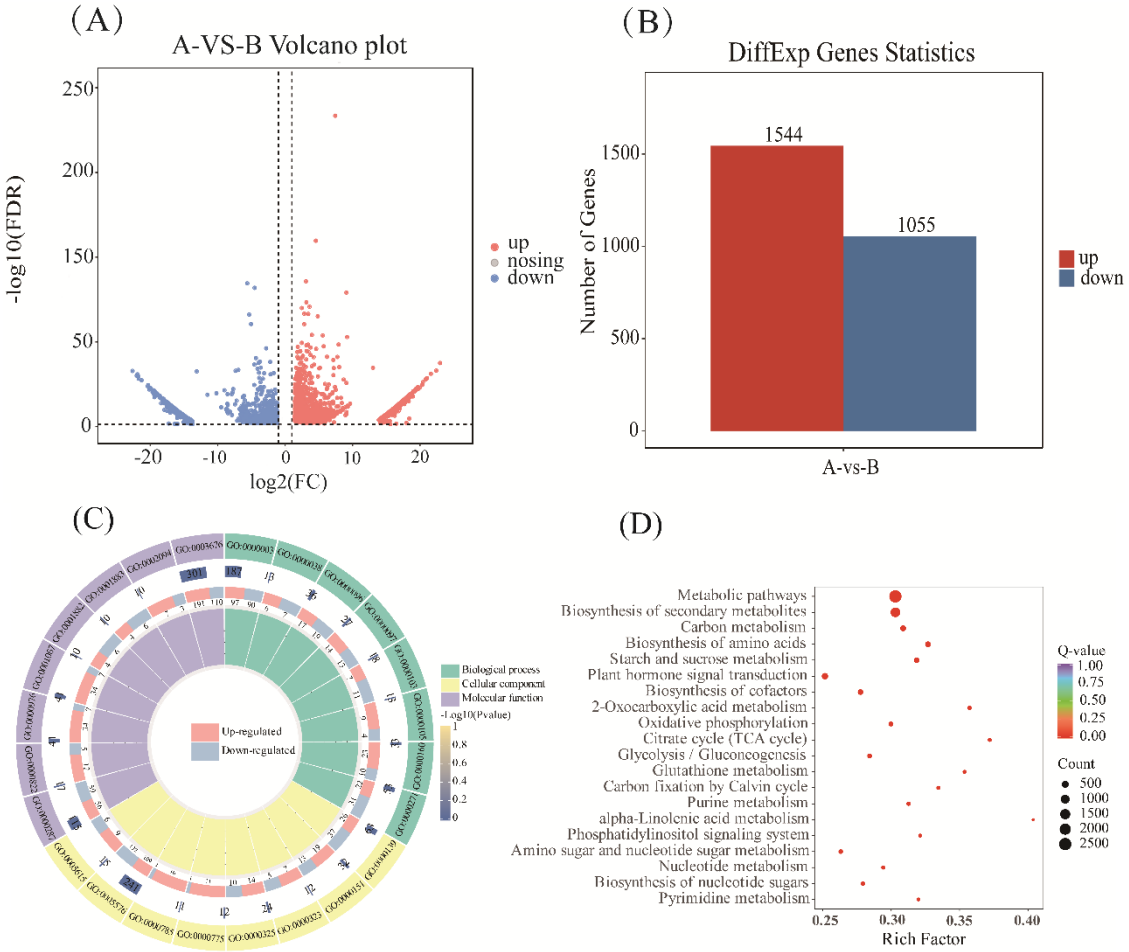

Figure 3. *Analysis of differential genes and functional analysis between HBES and SXHZ. (A) Differential gene volcano plot. (B) Differential expression statistics. (C). Gene function enrichment. (D) Pathway enrichment of metabolism*

Gene co-expression and network analysis

To identify co-expressed gene modules, this study employed Weighted Gene Co-expression Network Analysis (WGCNA). A clustering dendrogram was constructed by calculating pairwise gene expression correlations, and modules were identified using the dynamic tree cutting method. Modules with module eigengene similarity ≥ 0.25 were merged, and each module was required to contain at least 50 genes. The results are shown in (*Fig. 4A*), where different colors represent distinct co-expression modules, and each gene was assigned to a specific module. These modules typically consist of genes functionally linked in biological processes or across tissues. The upper part of the dendrogram illustrates the genetic distance between genes (vertical axis), while the horizontal axis holds no specific biological meaning.

Nine co-expression modules related to biological traits were obtained. Among them, the MEturquoise module (containing 3134 genes) and the MEblue module (containing 1958 genes) exhibited a clear antagonistic regulatory pattern: the MEblue module showed a strong positive correlation with eight phenotypic traits, including mws0192, whereas the MEturquoise module demonstrated a significant positive correlation with eleven metabolic characteristics, including pme3096 (*Fig. 4B, C*). To investigate the reason for

http://www.aloki.hu ● ISSN 1589 1623 (Print) ● ISSN 1785 0037 (Online)
DOI: http://dx.doi.org/10.15666/aeer/2402_19191936

this inverse correlation in gene expression between the aforementioned modules, we screened the top 20 hub genes in the MEblue module and the top 50 hub genes in the MEturquoise module based on their connectivity strengths (*Fig. 4D, E*). These highly connected genes are likely crucial components constituting this antagonistic network, providing high-value candidate targets for subsequent functional studies.

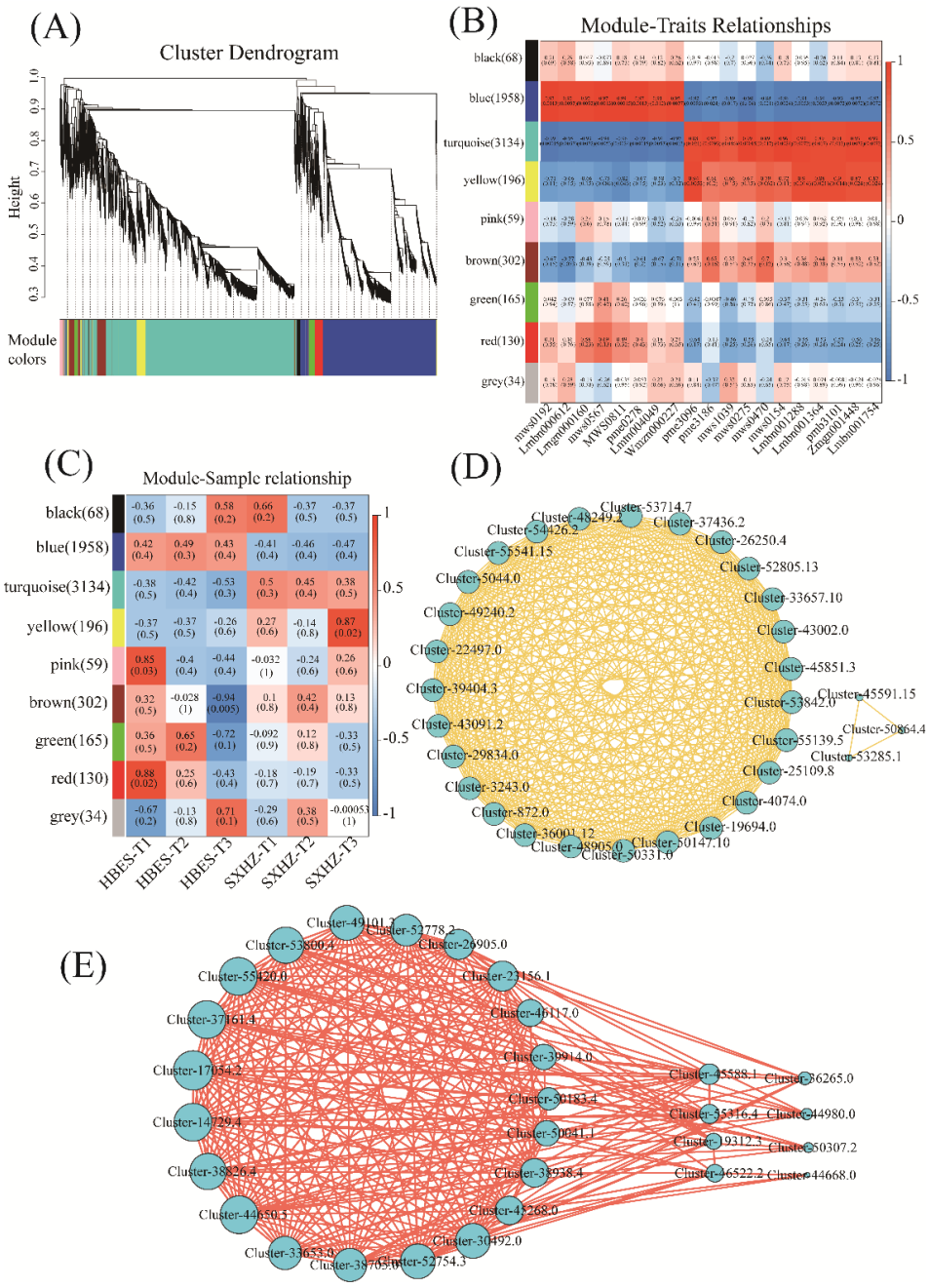

Figure 4. *HBES and SXHZ metabolic and transcriptomic correlation analysis. (A) Dendrogram showing co-expression modules identified by WGCNA. (B) Heatmap of module-metabolite correlations. Each row corresponds to a module labeled with different colors. Each column corresponds to a metabolite. Blue represents negative correlation. Red represents positive correlation. (C) Heatmap of module-HBES and module-SXHZ correlations. (D) Network plot showing the top 50 genes ranked by connection strength in the MEturquoise module. (E) Network plot illustrating the top 20 genes ranked by connection strength in the MEblue module*

http://www.aloki.hu ● ISSN 1589 1623 (Print) ● ISSN 1785 0037 (Online)
DOI: http://dx.doi.org/10.15666/aeer/2402_19191936

Integrated analysis of transcriptome and metabolome

To identify common genes regulating organic acid metabolism in the two *Polygonatum* varieties, we selected the top 10 differentially expressed genes (DEGs) based on correlation rankings and performed association analysis with the differential metabolites. The results showed that 10 genes, including Cluster-32977.1, exhibited significant positive correlations with the metabolites ($p < 0.05$), suggesting their potential key regulatory roles in organic acid metabolism. Further correlation analysis revealed that in SXHZ, the contents of shikimic acid (mws0154), DL-glyceraldehyde-3-phosphate (pme3186), and L-malic acid (mws0275) were significantly down-regulated, indicating these are key metabolic nodes responsible for the reduction in organic acid synthesis. In contrast, in HBES, succinic acid (mws0192) and abscisic acid (Lmtn004049) were significantly associated with increased organic acid content (*Fig. 5A, B*).

In a comparative analysis of organic acid biosynthesis pathways, we found that the changes in organic acids in HBES and SXHZ were closely related to aromatic amino acid biosynthesis and the TCA cycle. Specifically, the expression of genes encoding upstream enzymes such as DAHP synthase (EC 2.5.1.54) and 3-dehydroquinate synthase (EC 4.2.3.4) was down-regulated (highlighted in blue), leading to reduced carbon flux into the shikimic acid pathway. Conversely, genes encoding downstream branch enzymes like tryptophan synthase (EC 4.2.1.20) and prephenate dehydratase (EC 4.2.1.51) were up-regulated (highlighted in red), indicating a greater diversion of metabolic flux towards the synthesis of phenylalanine and tyrosine (*Fig. 6*).

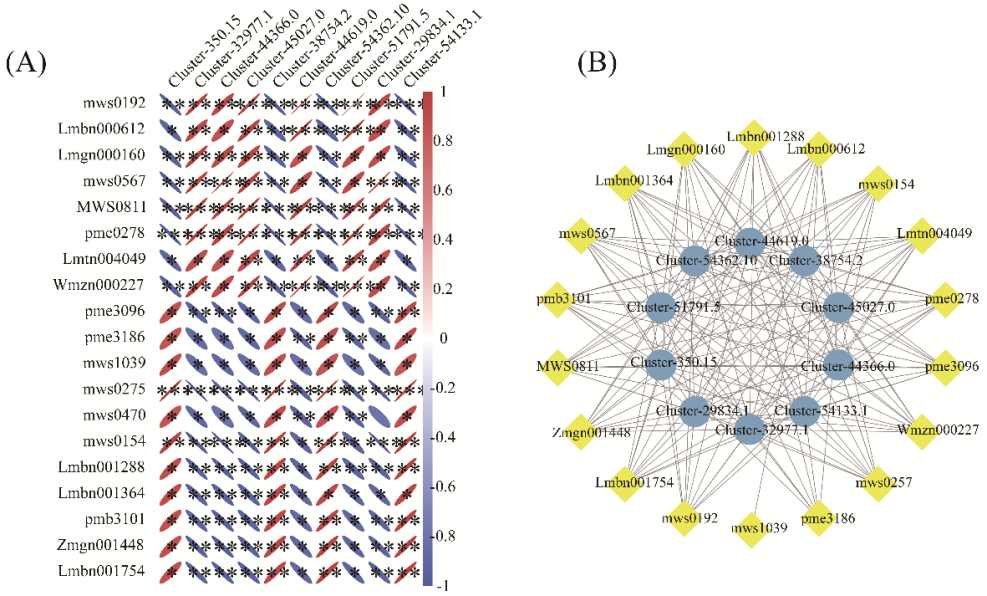

Figure 5. *Integrated analysis of differential genes and differential metabolites. (A) Heatmap of DEGs and DEMs involved in the organic acid biosynthesis pathway. colors and symbols indicate the strength and direction of the correlation, and the color bar on the right represents the range of correlation values, allowing you to visualize which samples are closely associated with a particular cluster. (B) Correlation network of the top 10 DEGs and all DEMs related to the organic acid biosynthesis pathway*

Integrated metabolomic and transcriptomic data analysis revealed that both differential metabolites and DEGs were co-enriched in pathways such as pyruvate metabolism, the

http://www.aloki.hu ● ISSN 1589 1623 (Print) ● ISSN 1785 0037 (Online)
DOI: http://dx.doi.org/10.15666/aeer/2402_19191936

TCA cycle, and aromatic amino acid biosynthesis. Genes encoding early enzymes of the shikimate pathway (e.g., DAHP synthase, DHQ synthase) showed negative correlations with down-regulated carbon source metabolites (e.g., G3P, E4P). In contrast, genes encoding specific downstream branch enzymes (e.g., tryptophan synthase and prephenate dehydratase) showed positive correlations with branch metabolites such as Phe and Tyr. These results demonstrate a coordinated pattern between gene expression and metabolite accumulation in the relevant pathways.

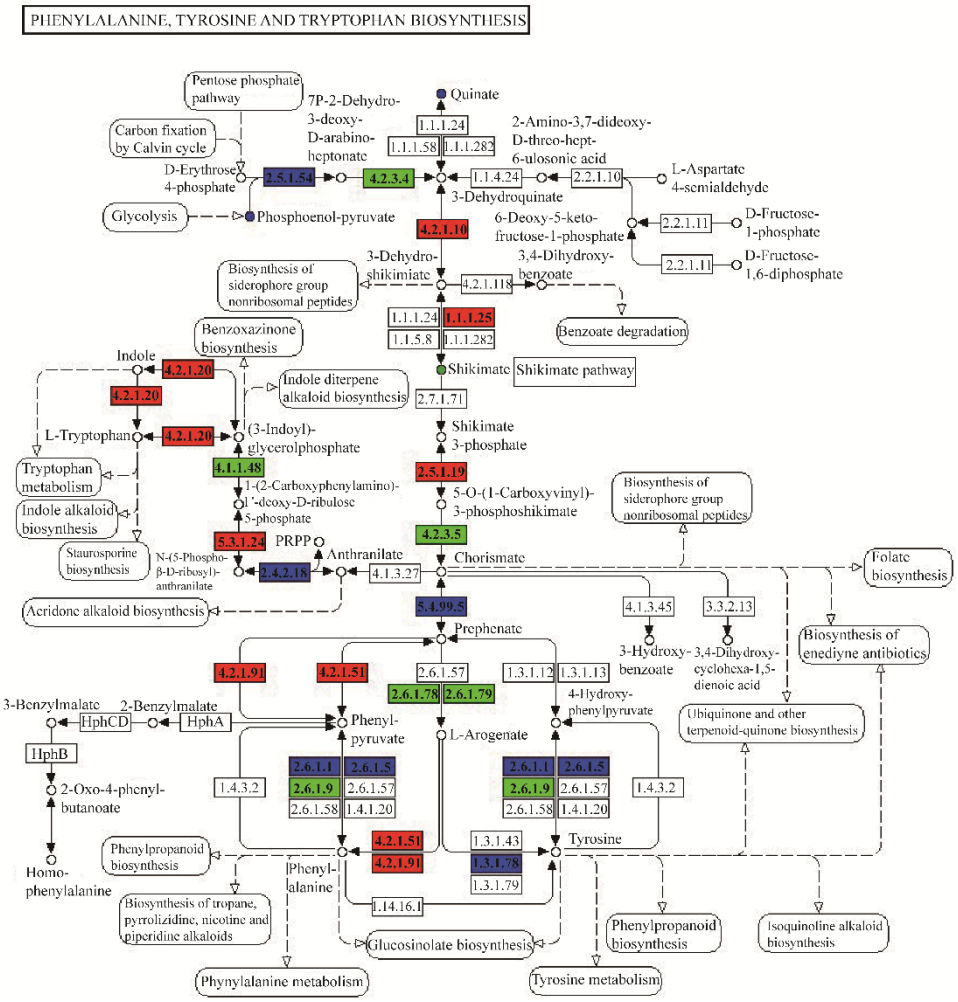

Figure 6. *Research on the biosynthesis and metabolism of organic acids in Polygonatum rhizome. Blue dots indicate metabolites detected but without significant changes, while green dots indicate that the content of metabolites in the experimental group is significantly downregulated. Red rectangles indicate that the enzyme is associated with upregulated genes, green rectangles indicate that the enzyme is associated with downregulated genes, and blue rectangles indicate that the enzyme is associated with both upregulated and downregulated genes. The numbers in the boxes represent enzyme numbers (EC numbers)*

Discussion

Organic acids, as crucial primary and secondary metabolites, play a central role in plant adaptation to the environment and in ecological strategies. They function not only as intermediates in energy metabolism but also as biostimulants and defense compounds,

http://www.aloki.hu ● ISSN 1589 1623 (Print) ● ISSN 1785 0037 (Online)
DOI: http://dx.doi.org/10.15666/aeer/2402_19191936

helping plants optimize resource allocation between growth and stress resistance (Quiroga et al., 2019). *Polygonatum* is a medicinal plant with significant cultivation value, and its metabolic characteristics are of great importance for achieving high-quality and high-yield cultivation (Xiao et al., 2024). However, the synergistic improvement of its medicinal quality and yield is constrained by various environmental factors (Hao et al., 2024). In this context, investigating the regulatory mechanisms of the organic acid metabolic network on the environmental adaptability and ecological fitness of Polygonatum is crucial for revealing the physiological basis of its varietal trait formation and for unlocking its economic and ecological potential under sustainable cultivation models (Chen et al., 2022).

Multiple studies have shown that organic acids function as biostimulants in plants, coordinating growth, development, and stress responses. For example, foliar application of succinic acid, malic acid, and oxalic acid in ryegrass significantly promotes plant growth, enhances root activity, and increases dry matter yield (Awad-Allah and Elsokkary, 2020); in aromatic plants such as parsley, pre-harvest spraying of citric acid and oxalic acid can also effectively improve their quality and antioxidant capacity (El-Zaeddi et al., 2017). Although these studies reveal the biostimulatory effects of organic acids, the underlying molecular mechanisms, particularly the main regulatory mechanisms by which specific organic acids influence plant growth, remain unclear. This study directly addresses this key scientific question by systematically analyzing the biosynthesis and regulatory networks of organic acid metabolites in HBES and SXHZ.

A total of 47 organic acids were identified in this study, which may exhibit growth-promoting and active-substance-accumulation patterns similar to those observed in ryegrass, suggesting that *Polygonatum* regulates endogenous growth mechanisms and adapts to external stress environments through organic acids. Metabolomic analysis further identified 19 differential metabolites (*Fig. 2C*). An in-depth comparison of their metabolic pathways revealed that the differential metabolites in the HBES ecotype are primarily involved in central carbon metabolism (ko00020), such as succinic acid, isocitric acid, and alpha-ketoglutaric acid (*Table 1*). Succinic acid can promote the synthesis of starch, proteins, and polysaccharides, facilitating rhizome expansion and dry matter accumulation, thereby enhancing yield and basic quality (Aslantas et al., 2017). Isocitric acid, catalyzed by isocitrate dehydrogenase, generates alpha-ketoglutaric acid and NADPH, which not only support fatty acid synthesis but also maintain antioxidant function, delaying oxidative damage and ensuring nutritional quality and post-harvest stability (Singh et al., 2022). Alpha-ketoglutaric acid serves as a precursor for amino acid synthesis and a key component of the GS/GOGAT pathway, promoting nitrogen assimilation and the formation of flavor compounds, while also regulating carbon-nitrogen balance and enhancing the plant's adaptability to low-nitrogen environments and resource allocation efficiency. These results indicate that the HBES ecotype has more active basal energy metabolism. In contrast, the differential metabolites in the SXHZ ecotype are more associated with stress response and secondary metabolic pathways (ko01100), such as jasmonic acid and phytic acid. These metabolites can enhance the plant's tolerance to various stresses, thereby improving its environmental adaptability and stress resistance (Chen et al., 2019).

Integrated transcriptomic and metabolomic data analysis revealed that shikimic acid (mws0154), DL-glyceraldehyde-3-phosphate (pme3186), and L-malic acid (mws0275) were significantly downregulated key differential metabolites in SXHZ. In contrast, succinic acid (mws0192) and abscisic acid (Lmtn004049) were significantly upregulated

http://www.aloki.hu ● ISSN 1589 1623 (Print) ● ISSN 1785 0037 (Online)
DOI: http://dx.doi.org/10.15666/aeer/2402_19191936

in HBES (*Fig. 5A*). We propose that the organic acid metabolic network in *Polygonatum* species exhibits significant species specificity. Its carbon flux distribution pattern is fundamentally different from that of traditional model plants. In most plants, central carbon metabolism typically coordinates energy production and carbon skeleton supply through the TCA cycle and the pentose phosphate pathway; whereas in *Polygonatum*, a unique carbon allocation strategy has evolved: after entering central metabolism, carbon flux exhibits ecotype-specific differentiation. Specifically, in the HBES ecotype, carbon metabolism is significantly biased toward the TCA cycle, with substantial accumulation of intermediates such as succinic acid and alpha-ketoglutaric acid, resulting in an "energy efficiency-oriented" metabolic mode. In contrast, the SXHZ ecotype directs carbon flux toward the synthesis of aromatic amino acids via the shikimate pathway, thereby enhancing the capacity for defense compound synthesis and constituting a "stress resistance-oriented" metabolic characteristic. The molecular basis of this metabolic differentiation lies in the differential expression of key node enzyme genes: genes related to the TCA cycle are significantly upregulated in HBES, while genes encoding downstream branching enzymes in the shikimate pathway are highly expressed in SXHZ, thereby directing the directional allocation of carbon flux and forming two distinct ecological adaptation strategies (*Fig. 5B*). The key genes screened in this study (such as Cluster-32977.1, etc.) may be core components of the regulatory network integrating environmental signals and carbon resource reallocation, influencing the ecological fitness of *Polygonatum* in specific habitats by regulating the dynamic balance of organic acids such as malic acid and succinic acid (*Fig. 6*). It is noteworthy that the native habitats of HBES and SXHZ are acidic soil and weakly alkaline soil, respectively. Although both have been co-cultivated under the same soil conditions for three years, their metabolic differences persist, indicating that these traits are genetically fixed. This not only suggests that the organic acid metabolic network is a core mechanisms of plant adaptation to soil environments but also implies that soil pH, as a key environmental selective pressure, has a decisive influence on the formation of metabolic networks in medicinal plants.

In summary, this study reveals the inherent differential metabolic strategies of two *Polygonatum* ecotypes from the perspective of organic acid metabolism. Current soil conditions do not directly drive these strategic differences. However, they are more likely to reflect fixed metabolic patterns shaped during their long-term adaptation to their respective native soil environments, such as differences in pH. Therefore, this research provides new evidence at the metabolic level for understanding plant resource allocation and adaptive evolution. The findings offer an important theoretical foundation and breeding direction for achieving "site-specific seed selection" and developing superior *Polygonatum* varieties with both high adaptability and high yield.

Conclusions

This study systematically revealed key differences in organic acid metabolic pathways between HBES and SXHZ through integrated metabolomic and transcriptomic analyses. A total of 47 organic acids and their derivatives were identified, among which 19 showed significant differences. Multivariate statistical analyses (PCA and OPLS-DA) demonstrated distinct separation in metabolite composition between the two varieties. Metabolomic data indicated significantly elevated levels of key intermediate metabolites —including succinic acid, isocitric acid, and α-ketoglutaric acid —in HBES, revealing enhanced central carbon metabolic flux that provides the metabolic foundation for its

http://www.aloki.hu ● ISSN 1589 1623 (Print) ● ISSN 1785 0037 (Online)
DOI: http://dx.doi.org/10.15666/aeer/2402_19191936

greater biomass accumulation. Transcriptome analysis further identified 10 core genes, including Cluster-32977.1, that showed significant correlations with organic acid metabolites, suggesting their crucial roles in the organic acid metabolic regulatory network. Future functional studies will focus on elucidating the specific roles of these genes in the synthesis of medicinal compounds and the regulation of growth environments in *Polygonatum*, thereby providing new targets and theoretical foundations for molecular breeding and pharmaceutical development of this medicinal plant.

Acknowledgements. I would like to express my sincere gratitude to my supervisor, Prof. Xiao Qiang, for his insightful guidance on the research direction and key issues of this work. I am also deeply thankful to Ms. Wang Xiuzhi for her selfless assistance in figure preparation and manuscript writing. Thank you both for your invaluable support.

Funding. This study was jointly supported by the National Natural Science Foundation of China (31260057), the Natural Science Foundation of Hubei Province (Joint Fund) (2023AFD077), the Central Special Fund for Guiding Local Science and Technology Development (Hubei Province) (2024BSB013), the Central Government Forestry Science and Technology Promotion Demonstration Project Fund (Hubei [2025] TG31), and the Hubei Provincial Key Laboratory of Biological Resources Conservation and Utilization (Hubei University for Nationalities).

REFERENCES

[1] Aslantas, R., Angin, I., Kose, M., Bernstein, N. (2017): Ethylenediamine-N,N-disuccinic acid mitigates salt-stress damages in strawberry by interfering with effects on the plant ionome. – Annals of Applied Biology 171(2): 190-201. https://doi.org/10.1111/aab.12364.

[2] Awad-Allah, E., Elsokkary, I. (2020): Influence of potassium nutrition and exogenous organic acids on iron uptake by monocot and dicot plants. – Open Journal of Soil Science 10: 486-500. https://doi.org/10.4236/ojss.2020.1010025.

[3] Azari, F., Vazirian, M., Shams Ardekani, M. R., Sharifzadeh, M., Sadati Lamardi, N. (2020): Hypoglycemic effect of Polygonatum orientale Desf. rhizome extract on diabetes induced by streptozotocin in rat model. – Journal of Medicinal Plants 19(75): 92-101. https://doi.org/10.29252/jmp.19.75.92.

[4] Chen, L., Xu, S., Liu, Y., Zu, Y., Zhang, F., Du, L., Chen, J., Li, L., Wang, K., Wang, Y., Chen, S., Chen, Z., Du, X. (2022): Identification of key gene networks controlling polysaccharide accumulation in different tissues of Polygonatum cyrtonema Hua by integrating metabolic phenotypes and gene expression profiles. – Frontiers in Plant Science 13: 1012231. https://doi.org/10.3389/fpls.2022.1012231.

[5] Chen, X., Wang, D. D., Fang, X., Chen, X. Y., Mao, Y. B. (2019): Plant specialized metabolism regulated by jasmonate signaling. – Plant and Cell Physiology 60(12): 2638-2647. https://doi.org/10.1093/pcp/pcz161.

[6] Chen, Y., Liu, J., Xu, Y., Sun, C., Qu, W., Du, H., He, M., Huo, J., Sun, J., Huang, J., Yin, J. (2024): Comparison of Polygonatum sibiricum polysaccharides found in young and mature rhizomes. – Foods 13(13): 2010. https://doi.org/10.3390/foods13132010.

[7] El-Zaeddi, H., Calín-Sánchez, Á., Nowicka, P., Martínez-Tomé, J., Noguera-Artiaga, L., Burló, F., Wojdyło, A., Carbonell-Barrachina, Á. A. (2017): Preharvest treatments with malic, oxalic, and acetylsalicylic acids affect the phenolic composition and antioxidant capacity of coriander, dill and parsley. – Food Chemistry 226: 179-186. https://doi.org/10.1016/j.foodchem.2017.01.067.

[8] Grabherr, M. G., Haas, B. J., Yassour, M., Levin, J. Z., Thompson, D. A., Amit, I., Adiconis, X., Fan, L., Raychowdhury, R., Zeng, Q., Chen, Z., Mauceli, E., Hacohen, N., Gnirke, A., Rhind, N., di Palma, F., Birren, B. W., Nusbaum, C., Lindblad-Toh, K.,

http://www.aloki.hu ● ISSN 1589 1623 (Print) ● ISSN 1785 0037 (Online)
DOI: http://dx.doi.org/10.15666/aeer/2402_19191936

Friedman, N., Regev, A. (2011): Full-length transcriptome assembly from RNA-Seq data without a reference genome. – Nature Biotechnology 29(7): 644-652. https://doi.org/10.1038/nbt.1883.

[9] Guan, Y., Liang, Z., Li, R., Guo, Y., Dang, L., Gong, F., Xu, S., Wang, T., Bo, N., Yang, S., Jiang, W., Zhang, G., Zhao, M., Chen, J. (2024): Chemical composition and antioxidant activity of Polygonatum kingianum processed by the traditional method of 'Nine Cycles of Steaming and Sun-Drying'. – Food Chemistry X 22: 101292. https://doi.org/10.1016/j.fochx.2024.101292.

[10] Hao, J. W., Fan, X. X., Li, Y. N., Chen, N. D., Ma, Y. F. (2024): Differentiation of Polygonatum cyrtonema Hua from different geographical origins by near-infrared spectroscopy with chemometrics. – Journal of AOAC International 107(5): 801-810. https://doi.org/10.1093/jaoacint/qsae036.

[11] Kanehisa, M., Furumichi, M., Sato, Y., Kawashima, M., Ishiguro-Watanabe, M. (2023): KEGG for taxonomy-based analysis of pathways and genomes. – Nucleic Acids Research 51(D1): D587-D592. https://doi.org/10.1093/nar/gkac963.

[12] Lai, W., Ning, Q., Wang, G., Gao, Y., Liao, S., Tang, S. (2024): Antitumor activity of Polygonatum sibiricum polysaccharides. – Archives of Pharmacal Research 47: 696-708. https://doi.org/10.1007/s12272-024-01511-3.

[13] Langfelder, P., Horvath, S. (2008): WGCNA: an R package for weighted correlation network analysis. – BMC Bioinformatics 9: 559. https://doi.org/10.1186/1471-2105-9-559.

[14] Li, D., Wang, Q., Chen, S., Liu, H., Pan, K., Li, J., Luo, C., Wang, H. (2022): De novo assembly and analysis of Polygonatum cyrtonema Hua and identification of genes involved in polysaccharide and saponin biosynthesis. – BMC Genomics 23: 195. https://doi.org/10.1186/s12864-022-08421-y.

[15] Liao, W. C., Huang, J. P., Huang, W. Y. (2023): Chemical composition analysis and biofunctionality of polygonatum sibiricum and Polygonatum odoratum extracts. – Archives of Pharmacal Research 18: 3608-3619. https://doi.org/10.15376/biores.18.2.3608-3619.

[16] Love, M. I., Huber, W., Anders, S. (2014): Moderated estimation of fold change and dispersion for RNA-seq data with DESeq2. – Genome Biology 15(12): 550. https://doi.org/10.1186/s13059-014-0550-8.

[17] Ma, W., Li, Y., Nai, G., Liang, G., Ma, Z., Chen, B., Mao, J. (2022): Changes and response mechanism of sugar and organic acids in fruits under water deficit stress. – PeerJ 10: e13691. https://doi.org/10.7717/peerj.13691.

[18] Mo, X., Wang, L., Yu, C., Kou, C. (2024): Combined metabolomics and transcriptomics analysis of the distribution of flavonoids in the fibrous root and taproot of Polygonatum kingianum Coll.et Hemsl. – Genes 15(7): 828. https://doi.org/10.3390/genes15070828.

[19] Morgunov, G., Kamzolova, S. V., Dedyukhina, E. G., Chistyakova, T. I., Lunina, J. N., Mironov, A. A., Stepanova, N. N., Shemshura, O. N., Vainshtein, M. B. (2017): Application of organic acids for plant protection against phytopathogens. – Applied Microbiology and Biotechnology 101: 921-932. https://doi.org/10.1007/s00253-016-8067-6.

[20] Ning, L., Xiao, Q., Tan, C., Gong, L., Liu, Y., Wang, Z., He, S., He, C., Yuan, H., Wang, W. (2024): An integrated targeted metabolome of phytohormones and transcriptomics analysis provides insight into the new generation of crops: Polygonatum kingianum var. grandifolium and Polygonatum kingianum. – Frontiers in Plant Science 15: 1464731. https://doi.org/10.3389/fpls.2024.1464731.

[21] Quiroga, P. R., Nepote, V., Baumgartner, M. T. (2019): Contribution of organic acids to α-terpine antioxidant activity. – Food Chemistry 277: 267-272. https://doi.org/10.1016/j.foodchem.2018.10.100.

[22] R Core Team (2023): R: A Language and Environment for Statistical Computing. – R Foundation for Statistical Computing, Vienna, Austria. https://www.R-project.org/.

[23] Schwachtje, J., Fischer, A., Koehl, K. (2018): Primed primary metabolism in systemic leaves: a functional systems analysis. – Scientific Reports 8: 216.

http://www.aloki.hu ● ISSN 1589 1623 (Print) ● ISSN 1785 0037 (Online)
DOI: http://dx.doi.org/10.15666/aeer/2402_19191936

https://doi.org/10.1038/s41598-017-18397-5.
[24] Shannon, P., Markiel, A., Ozier, O., Baliga, N. S., Wang, J. T., Ramage, D., Amin, N., Schwikowski, B., Ideker, T. (2003): Cytoscape: a software environment for integrated models of biomolecular interaction networks. – Genome Research 13(11): 2498-2504. https://doi.org/10.1101/gr.1239303.
[25] Singh, M., Singh, P., Prasad, S. M. (2022): α-Ketoglutarate enhanced Solanum melongena L. growth: acceleration of nitrogen assimilating enzymes and antioxidant system under arsenate toxicity. – Journal of Plant Growth Regulation 41: 1699-1713. https://doi.org/10.1007/s00344-021-10405-3.
[26] Thévenot, E. A., Roux, A., Xu, Y., Ezanno, E., Junot, C. (2015): Analysis of the human adult urinary metabolome variations with age, body mass index, and gender by implementing a comprehensive workflow for univariate and OPLS statistical analyses. – Journal of Proteome Research 14(8): 3322-3335. https://doi.org/10.1021/acs.jproteome.5b00354.
[27] Wang, S., He, F., Xiao, Y., Xiang, F., Lu, L., Wu, W., Ho, C., Li, S. (2024): Bioactive phytochemicals and associated multifunctional health-promoting effects of Polygonati Rhizoma. – Food Science and Human Wellness 14(6): 9250126. https://doi.org/10.26599/FSHW.2024.9250126.
[28] Wang, X. L., Cheng, Y. N., Zheng, B., Chen, Y., Xie, J. H., Hu, X. B., Qin, X. T., Song, J. J., Qiu, Y., Yu, Q. (2024): Effects of nine-steam-nine-bask processing on the bioactive compounds content, bioaccessibility, and antioxidant capacity of Polygonatum cyrtonema Hua. – Journal of Functional Foods 117: 106236. https://doi.org/10.1016/j.jff.2024.106236.
[29] Xiao, L., Xu, H., Wu, T., Xie, Q., Wen, R., Wang, L., Su, B., Zhang, H. (2024): Metabolomic diversity in Polygonatum kingianum across varieties and growth years. – Molecules 29(21): 5180. https://doi.org/10.3390/molecules29215180.
[30] Yu, J., Zhao, L., Wang, Z., Yue, T., Wang, X., Liu, W. (2024): Correlations between the structure and anti-diabetic activity of novel polysaccharides from raw and "Nine Steaming Nine Sun-Drying" Polygonti rhizome. – International Journal of Biological Macromolecules 260: 129171. https://doi.org/10.1016/j.ijbiomac.2023.129171.
[31] Zhang, X., Chen, Q., Chen, L., Chen, X., Ma, Z. (2024): Anti-aging in Caenorhabditis elegans of polysaccharides from Polygonatum cyrtonema Hua. – Molecules 29(6): 1276. https://doi.org/10.3390/molecules29061276.

http://www.aloki.hu ● ISSN 1589 1623 (Print) ● ISSN 1785 0037 (Online)
DOI: http://dx.doi.org/10.15666/aeer/2402_19191936